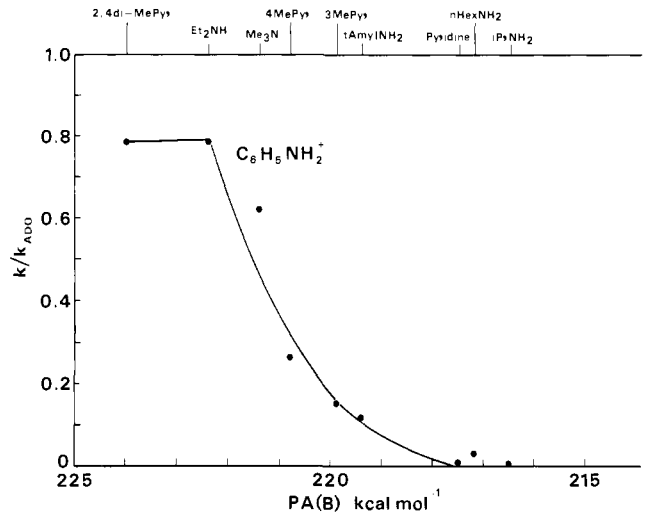

Figure 3. Reaction efficiencies as measured by k/k_{ADO} vs. proton affinities of reference bases, for $RH^+ + B \rightarrow BH^+ + R\cdot$, where RH^+ is the aniline ion; bases indicated on upper abscissa.

without complications. Rate constants and reaction efficiencies are given in Table III.

The reaction efficiencies as a function of PA(B) are given in Figure 3. Proton affinities of the reference bases were obtained using relative gas-phase basicities of amines and pyridines by Aue and Bowers.[10] Entropy considerations were handled as above, except that small entropy corrections were made owing to changes in σ_{rot} of the amine group due to protonation. The absolute PA values were related to the PA of n-Pr_2O as above.

From the falloff curve of Figure 3 we obtain $PA(C_6H_5NH\cdot) = 221.5$ kcal mol^{-1}. Equation 5 then gives $D°(C_6H_5NH-H) = 85.1$ kcal mol^{-1}. The difference between $D°(CH_3NH-H)$[20] and $D°(C_6H_5NH-H)$, due to resonance stabilization of the $C_6H_5NH\cdot$ radical, is 12 kcal mol^{-1}. This is similar to the resonance stabilization of $C_6H_5CH_2\cdot$, as compared with $CH_3CH_2\cdot$, which is about 14 kcal mol^{-1}.[21]

Acknowledgment. The author thanks Dr. P. Ausloos for suggesting this problem, and Drs. P. Ausloos and S. G. Lias for their continued interest and many helpful discussions during this work.

Registry No. Pyridine, 110-86-1; 3-methylpyridine, 108-99-6; 4-methylpyridine, 108-89-4; 2,4-dimethylpyridine, 108-47-4; *sec*-Bu_2O, 6863-58-7; *i*-Pr_2O, 108-20-3; *n*-Bu_2O, 142-96-1; MeO-*t*-Bu, 1634-04-4; *n*-Pr_2O, 111-43-3; Et_2CO, 96-22-0; MeCO-*i*-Pr, 563-80-4; MeCOOEt, 141-78-6; Et_2O, 60-29-7; EtCOOMe, 554-12-1; MeCOEt, 78-93-3; THF, 109-99-9; MeCOOMe, 79-20-9; $C_6H_5CH_3^+$, 34504-47-7; $C_6H_5CD_3^+$, 38091-11-1; $3\text{-}FC_6H_4CH_3^+$, 58436-59-2; $C_6H_5C_2H_5^+$, 39600-67-4; $C_6H_5C_3H_7^+$, 53649-54-0; $C_6H_5\text{-}i\text{-}C_3H_7^+$, 68199-09-7; $C_6H_5CH_2\cdot$, 2154-56-5; $3\text{-}FC_6H_4CH_2\cdot$, 2599-73-7; $C_6H_5\dot{C}HCH_3$, 2348-51-8; $C_6H_5\dot{C}HCH_2CH_3$, 19019-92-2; $C_6H_5\dot{C}(CH_3)_2$, 4794-07-4; $C_6H_5NH\cdot$, 2348-49-4; $C_6H_5CH_3$, 108-88-3; $C_6H_5CD_3$, 1124-18-1; $3\text{-}FC_6H_4CH_3$, 352-70-5; $C_6H_5C_2H_5$, 100-41-4; $C_6H_5\text{-}n\text{-}C_3H_7$, 103-65-1; $C_6H_5\text{-}i\text{-}C_3H_7$, 98-82-8; $C_6H_5NH_2$, 62-53-3; $i\text{-}PrNH_2$, 75-31-0; $n\text{-}hexNH_2$, 111-26-2; $t\text{-}amylNH_2$, 594-39-8; Me_3N, 75-50-3; Et_2NH, 109-89-7; $n\text{-}Pr_2OH^+$, 17009-84-6; $n\text{-}Bu_2OH^+$, 17009-85-7; $i\text{-}Pr_2OH^+$, 17009-86-8; *t*-Bu_2O, 6163-66-2; $C_6H_5\text{-}t\text{-}C_4H_9$, 98-06-6; $C_6H_5NH_2^+$, 34475-46-2; *t*-Bu^+, 14804-25-2.

Electron Spin Echo Studies of Cholestane Nitroxide Motion in Lecithin Multibilayer Dispersions and Vesicles: Detection of Nitroxide Probe Motion and Vesicle Rotation

Keith Madden,[1] Larry Kevan,*[2] Philip D. Morse II,[3] and Robert N. Schwartz[4]

Contribution from the Departments of Chemistry and Biological Sciences, Wayne State University, Detroit, Michigan 48202, Department of Chemistry, University of Houston, Houston, Texas 77004, and Department of Chemistry, University of California, Los Angeles, California 90024. *Received May 4, 1981*

Abstract: Electron spin echo spectroscopy has been used to *directly* measure the electron spin transverse relaxation time T_2 vs. temperature of the 3-doxyl-5α-cholestane nitroxide spin probe in egg yolk lecithin vesicles. In a preliminary study of cholestane nitroxide in isotropic liquids and in egg yold lecithin multibilayer dispersions (*J. Phys. Chem.* **1980**, *84*, 2691), the electron spin echo decay function was a single exponential attributed to motion of the spin probe. In contrast, the echo decay in vesicles exhibits fast and slow exponential decay components associated with spin probes with their long axes perpendicular and parallel to the magnetic field. In addition a new fast component appears at high temperatures which is attributed to vesicle rotation which moves a population of slowly relaxing spin probes into an orientation having faster relaxation. This appears to be the first *direct* observation of vesicle rotation by electron magnetic resonance.

The study of molecular motion in organized molecular assemblies such as bilayers, micelles, and vesicles is of considerable importance in understanding their biological and chemical functions. These systems have been extensively studied by incorporating paramagnetic probes and by using continuous wave electron spin resonance (CW ESR) to indirectly deduce the electron spin transverse relaxation time T_2 of the probe molecule.[5] T_2 is the reciprocal half-width at half-height of a *homogeneously* broadened ESR line and contains information on the motion of the probe. Unfortunately, the ESR resonances of nitroxide spin probes are inhomogeneously broadened by unresolved intramolecular hyperfine interactions[6] and a detailed knowledge of the magnitude of these interactions along with iterative spectral simulation procedures are required to obtain an estimate of T_2.[6-8]

(1) Radiation Laboratory, University of Notre Dame, Notre Dame, IN 46556.
(2) Wayne State University and University of Houston.
(3) Department of Biological Sciences, Wayne State University.
(4) On leave from the Department of Chemistry, University of Illinois at Chicago Circle, Chicago, IL 60680.

(5) Berliner, L. J. Ed. "Spin Labeling Theory and Applications"; Academic Press: New York, 1976.
(6) Stillman, A. E.; Schwartz, R. M. *J. Magn. Reson.* **1976**, *22*, 269.

0002-7863/82/1504-0010$01.25/0

Furthermore, additional complications occur for highly ordered hydrophobic nitroxide spin probes in oriented phospholipid bilayers due to inhomogeneous line width contributions from *bilayer heterogeneity*.[9]

Direct measurement of T_2 is possible, however, by using the electron spin echo (ESE) time domain ESR technique.[10] Irradiation of the spin system with a $\pi/2-\tau-\pi$ microwave pulse sequence where τ is the interpulse time generates an echo at time τ after the π pulse. The amplitude of the echo decays with τ as $\exp(-\tau/T_m)$ where $T_m = T_2/2$ for paramagnetic species undergoing rapid motion as typically found in the liquid phase. Recent experiments on nitroxide spin probes in toluene-d_8 confirm that the CW and ESE techniques yield equivalent values of T_2. In a previous communication[12] we reported the temperature dependence of T_2 for the cholestane nitroxide spin probe in decane, hexadecane, and egg yolk lecithin multibilayer dispersions. In all cases a single exponential decay curve was observed. In this work we extend our measurements to the cholestane nitroxide probe incorporated in egg yolk lecithin vesicles. The results show that the anisotropy of the nitroxide magnetic parameters can be detected in the echo decay curve.

Experimental Section

Egg yolk lecithin in chloroform (Sigma Chemical Co.) and 3-doxyl-5α-cholestane (Molecular Probes, Inc.) were used without further purification. All steps in the sample preparation were carried out in a nitrogen atmosphere by using nitrogen-bubbled reagents. The doxyl cholestane (cholestane nitroxide) was dissolved in chloroform and a 0.5 mol % spin probe to lipid ratio was typically prepared. This solution was evaporated to dryness at 40 °C in a rotary evaporator to form a uniform film on the walls of a 5-mL flask. Further drying overnight on a high vacuum line was necessary to completely remove solvent. The lipid film was redissolved to a concentration of 100 mg/mL by adding 0.1 M NaCl with 50 mM Tris buffer to the rotary evaporator flask and rotating at 40 °C. This gives a turbid multibilayer dispersion consisting of multiconcentric, multibilayer structures with a broad size distribution.[13] Single bilayer vesicles are formed from this solution by sonication at room temperature with a 300-W Artek sonicator equipped with a microprobe and operated at 35% power for 10 min until the solution becomes clear. The vesicle size and homogeneity were not independently monitored. This solution can then be centrifuged at 4 °C for 15 min at 48 000 G although deletion of this step had little effect. The clear solution is poured off and further degassed with nitrogen bubbling. Samples are prepared in a glovebox under nitrogen in 1-mm i.d. Pyrex capillary tubes filled by capillary action and quickly flame sealed. Three tubes were cemented to a microscope slide cover slip to create a flat cell.

Two pulse ($\pi/2-\tau-\pi$) ESE decay curves were recorded with a home-built X-band ESE spectrometer.[14] Typical pulses were 10 and 20 ns at 250 W. In liquids the free induction decay tends to obscure the echo signal. This interference was overcome by decreasing the homogeneity of the external magnetic field with a judiciously placed Allen wrench on one pole face. This shortens the free induction decay time so it does not interfere with the echo. In general, the echoes were weak and a typical decay curve required about 30 min to collect. However, the trends were reproducible in triplicate sample preparations. The temperature was controlled with a Varian E-4540 variable-temperature accessory and was measured to ±0.3 C with a copper–constantan thermocouple just above the active volume of the microwave cavity.

Results

Two pulse echoes were obtained from the $M_1 = 0$ ^{14}N hyperfine transition of the nitroxide ESR spectrum, as the echoes from $M_1 = \pm 1$ lines were too weak to measure over a significant range of

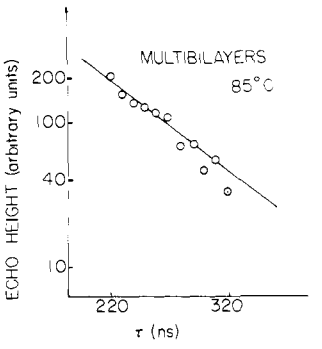

Figure 1. Electron spin echo decay curve of log (echo height) vs. interpulse time τ for 0.5 mol % cholestane nitroxide in an egg yolk lecithin multibilayer dispersion at 85 °C.

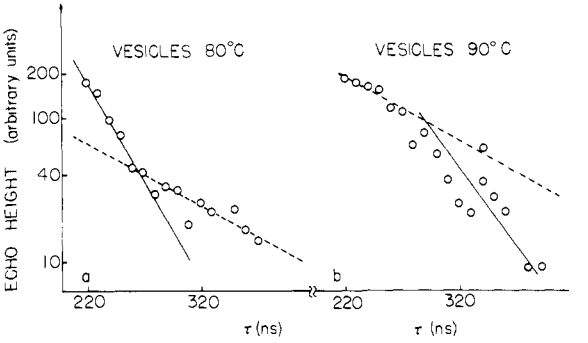

Figure 2. Electron spin echo decay curves of log (echo height) vs. interpulse time τ for 0.5 mol % cholestane nitroxide in egg yolk lecithin vesicles at (a) 80 °C and (b) 90 °C.

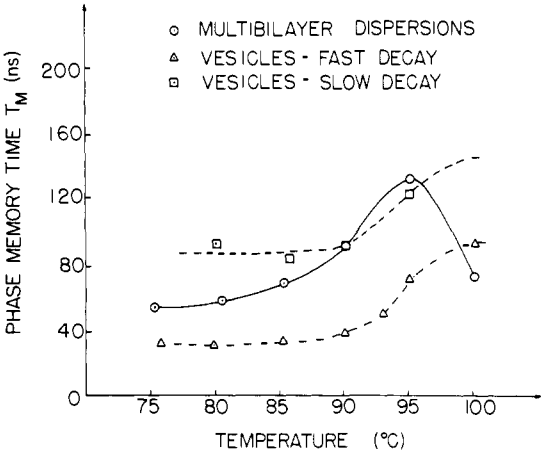

Figure 3. Temperature dependence of the electron spin echo phase memory time T_M for 0.5 mol % cholestane nitroxide in egg yolk lecithin multibilayer dispersions and vesicles. The points at 76 and 80 °C for the fast decay in vesicles correspond to fast components at the earliest observation times of the echo decay while the points at 85 °C and above correspond to fast components at the later observation times of the echo decay (see text). The error in T_M for a given preparation is about the height of the data points.

τ. As in the multibilayer dispersion studies,[12] strong echoes were found only at temperatures above 75 °C. While the multibilayer dispersions exhibited echoes with a single exponential decay, the vesicles showed a two component exponential decay as compared in Figures 1 and 2. The errors for a given sample preparation are less than the size of the experimental points. The lines drawn are least-squares fits with double weighting given to the first half of the points. The echo decay curves for vesicles in the temperature range 75–85 °C show an initial fast decay followed by a slower decay while from 85 to 100 °C an initial slow decay is followed by a fast decay. Two components can still be discerned at 85 °C although the fast decay predominates. Each fast and slow decay process can be characterized by a T_M value, the time for the echo

(7) Hwang, J. S.; Mason, R. P. 1 Hwang, L. P.; Freed, J. H. *J. Phys. Chem.* **1975**, *79*, 489.
(8) (a) Bales, B. L. *J. Magn. Reson.* **1980**, *38*, 193. (b) Salikhov, K. M.; Tsvetkov, Yu, D. In "Time Domain Electron Spin Resonance"; Kevan, L.; Schwartz, R. N., Eds.; Wiley-Interscience: New York, 1979; Chapter 7.
(9) Meirovitch, E.; Freed, J. H. *J. Phys. Chem.* **1980**, *84*, 3281.
(10) Stillman, A. E.; Schwartz, R. N. In "Time Domain Electron Spin Resonance"; Kevan, L.; Schwartz, R. N., Eds.; Wiley-Interscience: New York, 1979; Chapter 5.
(11) Schwartz, R. N.; Jones, L. L.; Bowman, M. K. *J. Phys. Chem.* **1979**, *83*, 3427.
(12) Madden, K.; Kevan, L.; Morse, P. D. II; Schwartz, R. N. *J. Phys. Chem.* **1980**, *84*, 2691.
(13) Huang, C. *Biochemistry* **1969**, *8*, 344.
(14) Ichikawa, T.; Kevan, L.; Narayana, P. A. *J. Phys. Chem.* **1979**, *83*, 3378.

intensity to fall to e^{-1} of its original value. These are shown in Figure 3 vs. temperature for the multibilayer dispersion decay and for the fast and slow components of the vesicle echo decay.

Discussion

A. Comparison of Multibilayers and Vesicles. The important new result in this work is the observed difference in the electron spin echo decay curves for the cholestane nitroxide spin probe in multibilayer dispersions and vesicles. This difference must be related to distinct differences in the local environment of the spin probe in these two types of sample preparations. The multibilayer dispersions are in the form of large multiconcentric, multibilayer structures of micrometer size.[13] The degree of curvature is small, and the phospholipid molecules constituting the bilayers are relatively loosely packed. Sonication of turbid multibilayer dispersions produces a clear solution of small, roughly spherical vesicles with a typical radius of 12 nm.[13] With this radius only several times greater than the phospholipid molecules themseleves a significantly tighter molecular packing in the vesicles compared to the multibilayer dispersions is expected. It will be seen that our results are consistent with this hypothesis.

B. Magnetic Tensor Anisotropy and Relaxation Anisotropy. The anisotropy of the magnetic parameters of the cholestane nitroxide implies some anisotropy in its relaxation behavior if the molecule is well oriented. The conventional coordinate system for cholestane nitroxide[15] defines the long molecular axis as the y axis, the NO bond direction as the x axis, and the unpaired electron orbital as the z axis. The **g** tensor anisotropy is small with principal values of $g_{xx} \simeq 2.009$, $g_{yy} \simeq 2.006$, and $g_{zz} \simeq 2.002$. However, the hyperfine tensor anisotropy is much larger with principal values of $A_{xx} \simeq A_{yy} \simeq 0.6$ mT and $A_{zz} \simeq 3.2$ mT, and its motional modulation provides a main relaxation pathway. Thus, if cholestane nitroxide is well oriented in bilayer dispersions, one expects fast and slow magnetic relaxation processes due to its rotational motion with respect to an applied magnetic field, H_0. The fast process would arise from those molecules with their long axis (y axis) perpendicular to H_0 in which case rotation about the y axis produces a hyperfine field at the unpaired electron that rapidly fluctuates between 0.6 and 3.2 mT. The slow magnetic relaxation process would arise from those molecules with their long axis parallel to H_0 in which case rotation about this axis causes little change in the hyperfine field at the unpaired electron. Of course, we have seen that the electron spin echo results in the multibilayer dispersions show only a single exponential decay indicative of only a single rotational relaxation process. Thus the slow and fast relaxation processes discussed above appear to be averaged. This is quite reasonable if the cholestane nitroxide molecules not only rotate about their own long axis but also wobble or tumble in a cone around this axis with a cone angle of $\sim 60°$ or greater. In the limit of 90° cone angle we would have isotropic tumbling. This type of motion for cholestane nitroxide has been suggested for oriented multibilayers[16] and vesicles[17] on the basis of simulations of CW ESR line shapes.

Now, let us consider the ESE decay curves of cholestane nitroxide in the vesicles. Here, we do observe two exponential components in the decay curves indicative of anisotropic relaxation. At temperatures below 85 °C the echo decay vs. the interpulse time τ exhibits a fast decay at short τ and a slower decay at long τ. This behavior can be interpreted as due to two simultaneous rotational relaxation pathways of the cholestane nitroxide corresponding to the long molecular axis of rotation being perpendicular (fast process) and parallel (slow process) to H_0 as described above. The geometry of these two orientations is illustrated in Figure 4. In the small vesicle with denser molecular packing than the multibilayers the spin probe is more constrained in its motion and does not exhibit such a large conical tumbling as postulated for the multibilayers. Thus, in vesicles, anisotropy of the rotational relaxation of the spin probe is observed as expected on the basis of its anisotropic magnetic parameters and a preferred orientation.

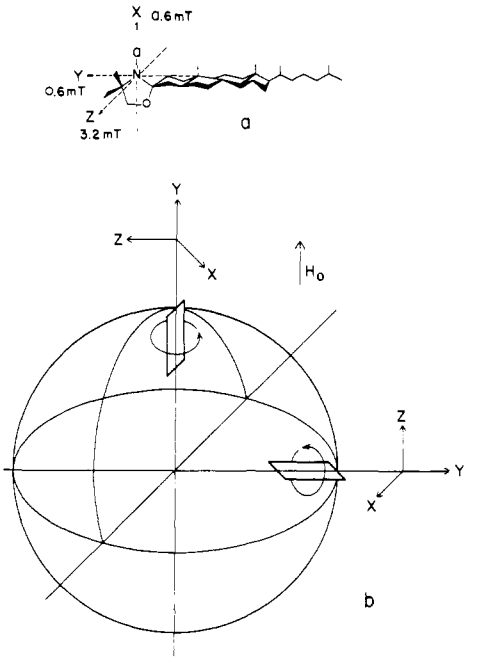

Figure 4. (a) Orientation of the nitrogen hyperfine tensor axes with respect to the molecular axes of cholestane nitroxide. The principal hyperfine values are also shown. (b) Axial and equatorial orientations of cholestane nitroxide in a lecithin vesicle in an axial magnetic field H_0. Rotation about the long molecular axis (y axis) produces fast relaxation for the equatorial orientation and slow relaxation for the axial orientation.

C. Evidence for Vesicle Rotation. An interesting anomalous feature of the two component ESE decay curves in vesicles occurs at 85 °C and above. In this temperature region the echo decay curve still shows two components, but now the slower decay occurs at shorter τ and the faster decay occurs at longer τ. This behavior cannot be explained in terms of simultaneous relaxation processes. Instead, it seems only explicable in terms of two populations of relaxing spins which are interconverted in a time dependent process. We postulate that this interconversion process is rotation of the entire vesicle. Figure 4 illustrates this picture which we will explicate in terms of increasing τ. Initially on a time scale less than that of vesicle rotation the simultaneous fast and slow relaxation processes that we have already described occur. However, we do not observe the fast process in this higher temperature range because it occurs within the 200-μs dead time of the ESE spectrometer response. Thus the slow relaxation process is initially observed at short τ. Now, when vesicle rotation occurs, it moves the spin probes parallel to H_0 which undergo slow relaxation to an orientation perpendicular to H_0 where they now undergo fast relaxation. Thus, at longer τ a fast relaxation process is observed in the echo decay curve due to this new population of spin probes which has been moved by vesicle rotation. The effect of this vesicle rotation is not observed at lower temperatures because the rotation is slower and the echo signal has reached the noise level before such effects can be seen.

The validity of this vesicle rotation model is supported by an estimate of the vesicle rotation time from the Debye equation for the rotation of a sphere in a viscous fluid. This equation[18] is

$$\tau_R = 4\pi r^3 \eta / 3k_B T \qquad (1)$$

where τ_R is the rotational correlation time, r is the radius of the sphere, η is the shear viscosity of the fluid, k_B is Boltzmann's constant, and T is the absolute temperature. The vesicle radius is about 12 nm, and η for water is 0.4042×10^{-2} P at $T = 343$

(15) Schreier, S.; Polnaszek, C.; Smith, I. C. P. *Biochim. Biophys. Acta* **1978**, *515*, 375.
(16) Shimoyama, Y.; Goran Eriksson, L. E.; Ehrenberg, A. *Biochim. Biophys. Acta* **1978**, *508*, 213.
(17) Israelachvili, J.; Sjosten, J.; Goran-Eriksson, L. E.; Ekstrom, M.; Graslund, A.; Ehrenberg, A. *Biochim. Biophys. Acta* **1975**, *382*, 125.
(18) Debye, P. "Polar Molecules" Dover Publications: New York, 1929; p 81.

K and 0.2975×10^{-2} P at 368 K.[19] For these values $\tau_R \approx 600$ ns at 70 °C and 400 ns at 95 °C. The breakpoint between the slow and fast components at 90 °C is ~300 ns which is in semiquantiative agreement with this idealized calculation for vesicle rotation. Recent deuterium nuclear magnetic resonance studies at room temperature have also indicated that vesicle rotation affects the nuclear transverse relaxation time.[20-22]

D. Temperature Dependence of T_M. Figure 3 shows the temperature dependence of T_M measured for the multibilayers and the vesicles. In the region from 75 to 85 °C the magnitude of T_M for the multibilayers is intermediate between the fast and slow decay values of T_M found in the vesicles. This is as expected if the cholestane nitroxide in the multibilayers undergoes wide angular excursions which average the intrinsic fast and slow decay values of T_M.

The increase of T_M with increasing temperature in the multibilayers has been explained as follows.[12] The hyperfine anisotropy becomes more averaged due to greater molecular reorientation at higher temperature and decreases the relaxation rate. Since T_M is proportional to T_2, we also note that a T_2 (or T_M) increase with temperature indicates that the electron spin relaxation phenomena can be described by a motionally narrowed formalism. A similar temperature dependence is observed for both the fast and slow decay components in the vesicles. However, the increase occurs at higher temperatures in the vesicles which is consistent with a more restrictive environment and greater molecular packing in the vesicles compared to the multibilayers.

In the highest temperature region shown in Figure 3, T_M reaches a maximum and then decreases with increasing temperature. This was previously interpreted for the multibilayer dispersions as the onset of spin dephasing by Heisenberg spin exchange due to increasing translational motion. This interpretation is supported by results on changing the nitroxide probe concentration by twofold in multibilayer dispersions which does affect T_M, particularly in the higher temperature range. An increased nitroxide probe concentration introduces the onset of spin exchange at lower temperatures and tends to partially cancel the increase of T_M with temperature observed at lower spin probe concentrations.

Conclusions

This work demonstrates that *directly* measured transverse electron relaxation times of nitroxide spin probes by time domain techniques can differ between multibilayer dispersions and vesicles. In particular, the anisotropy of the magnetic parameters of the nitroxide is averaged differently in these two types of model membrane preparations. Finally, evidence of vesicle rotation has been directly detected in electron spin echo decay curves.

Acknowledgment. This work was partially supported by NSF Grant INT77-21688. We thank Drs. V. Leon and B. Bales for helpful discussions.

Registry No. Cholestane nitroxide, 18353-76-9.

(19) Weast, R. C., Ed. "Handbook of Chemistry and Physics", 51st edition, CRC Press: Cleveland, OH, 1970; p F-36.
(20) Stockton, G. W.; Polnaszek, C. F.; Tulloch, A. P.; Hasan, F.; Smith, I. C. P. *Biochemistry* **1976**, *15*, 954.
(21) Bloom, M.; Burnell, E. E.; Mackay, A. L.; Nichol, C. P.; Valic, M. I.; Weeks, G. *Biochemistry* **1978**, *17*, 5750.
(22) Mackay, A. L.; Burnell, E. E.; Nichol, C. P.; Weeks, G.; Bloom, M.; Valic, M. I. *FEBS Lett.* **1978**, *88*, 97.

Electron Photodetachment Study of Sulfur Hexafluoride Anion: Comments on the Structure of SF_6^-

Paul S. Drzaic and John I. Brauman*

Contribution from the Department of Chemistry, Stanford University, Stanford, California 94305. *Received January 19, 1981*

Abstract: Electron photodetachment in the gas phase from the sulfur hexafluoride anion, SF_6^-, has been attempted. When using ion cyclotron resonance spectrometry to generate, trap, and detect ions, no observable photodetachment from SF_6^- was detected upon irradiation with visible light from either broad band arc lamp or laser sources. Theoretical cross-section calculations which have proven reliable in the past indicate that octahedral SF_6^- should possess a large cross section for photodetachment. A model consistent with the lack of photodetechment is one in which SF_6^- has a geometry distorted significantly from that of the neutral. This model is shown to be consistent with the observed kinetic barrier to electron transfer from SF_6^- in gas-phase ion–molecule reactions. Statistical rate theory is used to show that the predicted autodetachment lifetime of a loose, distorted SF_6^- is in the same range as that observed experimentally, while an SF_6^{-*} which resembles the parent neutral results in a predicted lifetime orders of magnitude too small. Two models consistent with this behavior are (1) an octahedral SF_6^- with sulfur–fluorine bonds weakened significantly from those in the neutral and (2) an SF_6^- that exists as an ion–molecule association complex, $(SF_5 \cdot F)^-$. Other negative ions besides SF_6^- also show behavior which may be explained by similar models. The usefulness of SF_6 as a dielectric material in high-voltage electrical equipment is related to its molecular properties.

The negative ion of sulfur hexafluoride, SF_6^-, has been the subject of intensive and continuing investigations. Sulfur hexafluoride has one of the largest low-energy electron-capture cross sections known;[1] it has found extensive applications as an electron scavenger in liquids and gases[2] and as a high-voltage dielectric material. It is probably the most extensively studied electron–molecule system. In spite of these studies, however, many of the properties of SF_6^- remain peculiar and inconsistent with what might be expected based on our knowledge of other negative ions. This paper describes our attempts to photodetach electrons from SF_6^-, and we suggest a model which accounts for the unusual properties of this ion.

It was shown[3] as early as 1953 that SF_6 is able to capture an electron nondissociatively to form SF_6^-, as well as to undergo a dissociative process to form $SF_5^- + F$. The parent ion, SF_6^-, has been observed by a variety of techniques. Among its peculiar

(1) Christophorou, L. G.; McCorkle, D. L.; Carter, J. G. *J. Chem. Phys.* **1971**, *54*, 253.
(2) (a) Bansal, K. M.; Fessenden, R. W. *J. Phys. Chem.* **1976**, *80*, 1743. (b) Chen, J. D.; Armstrong, D. A. *J. Chem. Phys.* **1968**, *48*, 2310.
(3) Ahearn, A. J.; Hannay, N. B. *J. Chem. Phys.* **1953**, *21*, 119.

0002-7863/82/1504-0013$01.25/0